View metadata, citation and similar papers at core.ac.uk
brought to you by CORE
provided by Elsevier - Publisher Connector

Available online at www.sciencedirect.com
ScienceDirect
Nuclear and Particle Physics Proceedings 273–275 (2016) 149–155
www.elsevier.com/locate/nppp

FCC study: parameters and optics for hadron and lepton colliders

R. Tomás[a], M. Benedikt[a], A.V. Bogomyagkov[b], L. Bottura[a], F. Cerutti[a], L.S. Esposito[a], A. Ferrari[a], B. Haerer[a,c], B. Holzer[a], E. Jensen[a], M. Koratzinos[a], R. Martin[a,d], L. Medina[a,e], D. Schulte[a], E. Todesco[a], J. Wenninger[a], S. White[f], F. Zimmermann[a]

[a] *CERN, Geneva, Switzerlan*
[b] *BINP, Novosibirsk, Russia*
[c] *Karlsruhe Institute of Technology, Germany*
[d] *Humboldt University Berlin, Germany*
[e] *Universidad de Guanajuato, México*
[f] *ESRF, Grenoble, France*

Abstract

A new international study has just been launched to design a hadron collider with a centre-of-mass energy of the order of 100 TeV in a new 80-100 km tunnel as a long-term goal. The design study includes a 90-350 GeV lepton collider, seen as a potential intermediate step, and an ep option. This paper reports on the overall parameters and preliminary optics designs with special emphasis on the Interaction Regions and the constraints arising for having to host both the lepton and the hadron colliders. Preliminary hardware specifications, as magnetic field, gradient, lengths and aperture are also presented.

1. Introduction

The Future Circular Collider (FCC) [1] design study aims at providing proton collisions with an energy about an order of magnitude beyond the existing Large Hadron Collider (LHC). Specifically, the FCC ring circumference of about 100 km (Fig. 1) would enable pp collisions of 50 TeV c.m. with the present 8.3 T LHC magnets, of 100 TeV with 16-T magnets (FCC-hh baseline), and of 125 TeV with 20-T magnets. The same tunnel infrastructure could accommodate a high-luminosity circular e^+e^- collider (FCC-ee), operating at 90–350 (500) GeV, as a potential intermediate step, and a high-luminosity high-energy lepton-hadron collider (FCC-he).

With a maximum centre-of-mass energy of 209 GeV, LEP2, in operation at CERN until 2001, has been the highest energy e^+e^- collider so far. The discovery, in 2012, of a Higgs-like boson at an energy reachable by a collider slightly more energetic than LEP2, together with the excellent performance achieved in the two B factories PEP-II and KEKB, have led to new proposals [2, 3, 4, 5, 6] for a next-generation circular e^+e^-

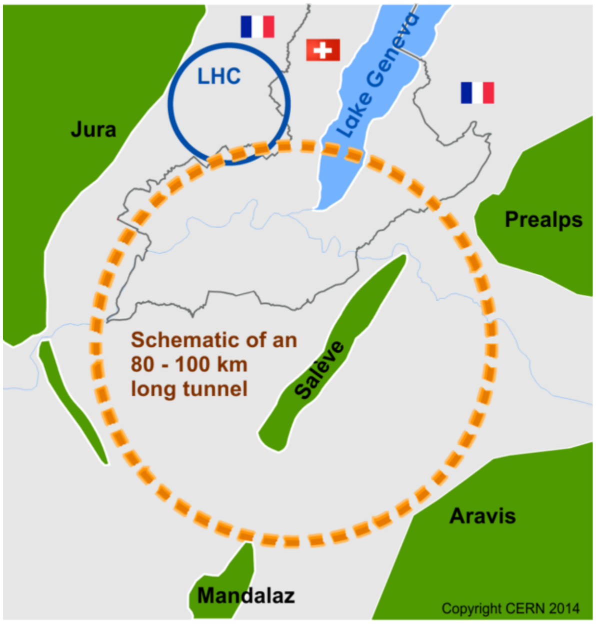

Figure 1: Schematic of a 100 km tunnel for a highest-energy circular collider in the Lake Geneva basin.

http://dx.doi.org/10.1016/j.nuclphysbps.2015.09.018
2405-6014/© 2015 Elsevier B.V. All rights reserved.

collider. In order to serve as a Higgs factory such a collider needs to be able to operate at least at a centre-of-mass energy of 240 GeV (for efficient $e^+e^- \rightarrow ZH$ production), i.e. 15% above the LEP2 peak energy. Reaching even higher energies, e.g. up to 350 GeV centre of mass, for $t\bar{t}$ production, or 500 GeV for ZHH and $Zt\bar{t}$ studies, might be possible for a new ring of larger circumference.

FCC-ee (formerly TLEP), a machine of 100 km circumference with 4 Interaction Points (IPs), aims at 2×10^{34} and 6×10^{34} cm^{-2}s^{-1} per IP at 350 and 240 GeV, respectively, as well as much higher luminosities at the Z pole and WW threshold, for high-precision measurements [7].

Table 1 compares the beam parameters of the proposed future circular colliders with the LHC design and LEP2, respectively.

2. The tunnel

The length of the FCC tunnel ranges between 80 and 100 km, see Fig. 1. Its shape could be close to circular, like the LHC, or could include long straight sections with various functionalities forming a racetrack, like the SSC. During the SSC design the racetrack shape was favoured from the beam dynamics point of view for having better control of the optics between adjacent Interaction Regions (IRs) placed in the same straight section [8, 9]. This would allow stable cancellations of chromatic aberrations between the IRs. Nevertheless, the LHC has demonstrated unprecendented optics control around the 27 km [10] for hadron colliders, reaching a peak relative beta-function deviation of 7 ± 4% throughout the machine cycle. This has been possible thanks to an excellent magnetic model [11] and the installation of AC dipoles [12] which allow using the same beam for several non-desctructive optics measurements [13].

In summary beam dynamics do not favour either the circular or the racetrack shape. So far, this is also true for the lepton collider. The tunnel shape should be decided from geological and infrastructural considerations.

3. Hadron Collider

FCC-hh major challenges include the development of economical high-field magnets; the arc beam pipe, which will be exposed to synchrotron-radiation (SR) levels unprecedented in a cold machine; the design of the interaction region for minimum β^*; and overall parameter optimization including constraints from the detectors.

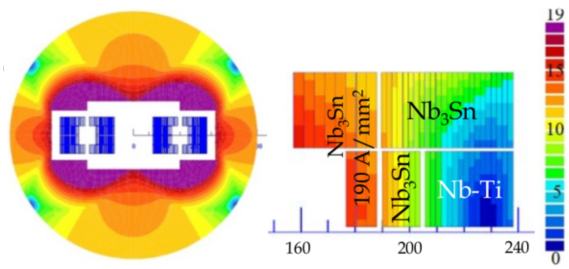

Figure 2: Preliminary design of the FCC-hh superconducting magnets, featuring a 30 cm beam separation and a field of 15 T [14].

The magnets of the present LHC are made from Nb-Ti superconductor, which supports a maximum field of about 10 T. Nb_3Sn superconductor can reach a practical magnetic field up to 16 T. The production of Nb_3Sn cables is well advanced, and the installation of a few Nb_3Sn dipole and quadrupole magnets is planned for the HL-LHC around 2023, which will represent an important milestone towards the FCC. A preliminary design of the FCC-hh dipoles at 15 T is shown in Fig. 2 [14].

The FCC-hh design baseline aims at a peak luminosity of 5×10^{34} cm^{-2}s^{-1}, i.e., the same value as for the LHC luminosity upgrade (HL-LHC). At 100 TeV with 25-ns bunch spacing this luminosity corresponds to a pile up of about 170 events per crossing, a beam lifetime of about 19 hours (with a total cross section $\sigma_{tot} \approx 153$ mbarn), and close to 100 kW of debris at each collision point.

Scaling, from the LHC, the arc longitudinal dimensions as the square root of the circumference yields an FCC-hh arc cell about 200 m long, a betatron tune around 120, and a maximum value of the arc beta functions of about 350 m. Similar values are derived from considerations of beam stability, dipole fill factor, and magnet-strength limitations.

In straight sections it is possible to scale the longitudinal dimensions with the third root of the energy. This is achieved by keeping constant the quadrupole pole tip field (assuming same technology), increasing the gradient and reducing the aperture by the same factor of the third root of the energy ratio. With this configuration the beta-function along the straigth section scales with the third root of the energy.

Scaling from the LHC, or the HL-LHC IR, the minimum required FCC IR length is $(50/7)^{1/3} \times 550$m$\approx$ 1100 m. This yields a β^* value of 0.8 m which provides margin to reach the FCC design of β^*=1.1 m, see Fig. 3.

Table 1: Parameters of the proposed FCC-hh, FCC-ee/TLEP, compared with LEP2 and the LHC design.

parameter	LHC (pp) design	FCC-hh	LEP2 achieved	FCC-ee (TLEP) Z	Z (cr. w.)	W	H	$t\bar{t}$
species	pp	pp	e^+e^-	e^+e^-	e^+e^-	e^+e^-	e^+e^-	e^+e^-
$E_{\rm beam}$ [GeV]	7,000	50,000	104	45.5	45	80	120	175
circumf. [km]	26.7	100	26.7	100	100	100	100	100
current [mA]	584	500	3.0	1450	1431	152	30	6.6
no. of bunches, n_b	2808	10600	4	16700	29791	4490	1360	98
N_b [10^{11}]	1.15	1.0	4.2	1.8	1.0	0.7	0.46	1.4
ϵ_x [nm]	0.5	0.04	22	29	0.14	3.3	0.94	2
ϵ_y [pm]	500	41	250	60	1	7	2	2
β^*_x [m]	0.55	1.1	1.2	0.5	0.5	0.5	0.5	1.0
β^*_y [mm]	550	1100	50	1	1	1	1	1
σ^*_x [μm]	16.7	6.8	162	121	8	26	22	45
σ^*_y [μm]	16.7	6.8	3.5	0.25	0.032	0.13	0.044	0.045
θ_c [mrad]	0.285	0.074	0	0	30	0	0	0
$f_{\rm rf}$ [MHz]	400	400	352	800	300	800	800	800
$V_{\rm rf}$ [GV]	0.016	>0.020	3.5	2.5	0.54	4	5.5	11
α_c [10^{-5}]	32	11	14	18	2	2	0.5	0.5
$\delta^{\rm SR}_{\rm rms}$ [%]	—	—	0.16	0.04	0.04	0.07	0.10	0.14
$\sigma^{\rm SR}_{z,\rm rms}$ [mm]	—	—	11.5	1.64	1.9	1.01	0.81	1.16
$\delta^{\rm tot}_{\rm rms}$ [%]	0.003	0.004	0.16	0.06	0.12	0.09	0.14	0.19
$\sigma^{\rm tot}_{z,\rm rms}$ [mm]	75.5	80	11.5	2.56	6.4	1.49	1.17	1.49
F_{hg}	1.0	1.0	0.99	0.64	0.94	0.79	0.80	0.73
$\tau_{\parallel}$ [turns]	10^9	10^7	31	1320	1338	243	72	23
ξ_x/IP	0.0033	0.005	0.04	0.031	0.032	0.060	0.093	0.092
ξ_y/IP	0.0033	0.005	0.06	0.030	0.175	0.059	0.093	0.092
no. of IPs, n_{IP}	3 (4)	2 (4)	4	4	4	4	4	4
L/IP [10^{34}/cm^2/s]	1	5	0.01	28	219	12	6	1.7
$\tau_{\rm beam}$ [min]	2760	1146	300	287	38	72	30	23
$P_{\rm SR}$/beam [MW]	0.0036	2.4	11	50	50	50	50	50
energy / beam [MJ]	392	8400	0.03	22	22	4	1	0.4

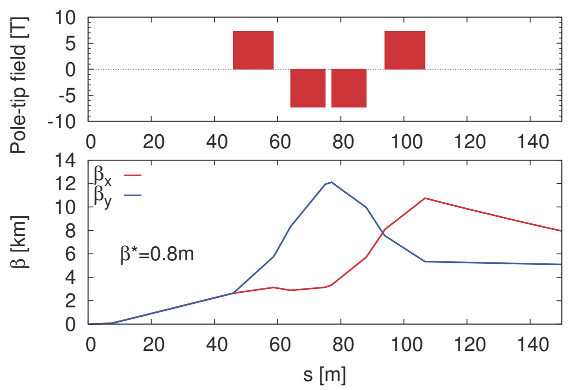

Figure 3: FCC-hh triplet design with $\beta^* = 0.8$ m and a free length of $L^*= 46$ m obtained by scaling the LHC triplet with the factor $(50/7)^{1/3}$.

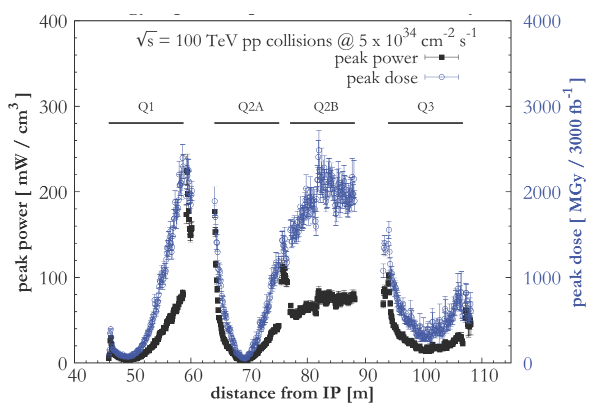

Figure 5: Energy deposition in the first FCC-hh triplet design.

Energy deposition simulations have been carried out for this triplet design. The corresponding FLUKA [15] model is shown in Fig. 4.

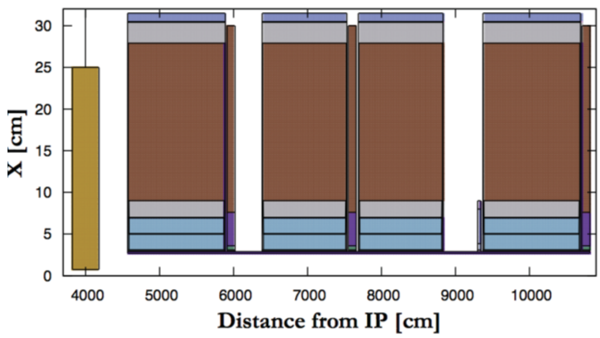

Figure 4: FLUKA model of the first FCC-hh tiplet design showing the TAS (yellow), superconducting coils (blue and green) and the iron yoke (brown).

The dose received by the triplet quadrupoles assuming a luminosity of $5 \times 10^{34}\text{cm}^{-2}\text{s}^{-1}$ is almost two orders of magnitude larger than that for the LHC, see Fig. 5. This would only allow to integrate 30 fb^{-1} assuming a larger resilience to radiation of the Nb_3Sn triplet quadrupoles.

In order to alleviate the radiation dose in the triplets it is necessary to increase the quadrupole aperture and increase the thickness of the absorbing material in between the coils and the beam pipe. This can be achieved by reducing the free distance to the IP and might, in principle, allow to reduce the β^*. Figure 6 shows a "pushed" IR optics which achieves a significantly lower β^* of 0.3 m with $L^*= 36$ m. This could allow reducing the beam current below its baseline value of 0.5 A, while keeping the peak or integrated luminosity constant. For example, with a β^* of 0.3 m, at equal average luminosity the maximum beam current would need to be only 0.20–0.25 A, instead of 0.5 A, reducing the SR power by more than a factor of two. The energy deposition studies for this pushed IR are underway.

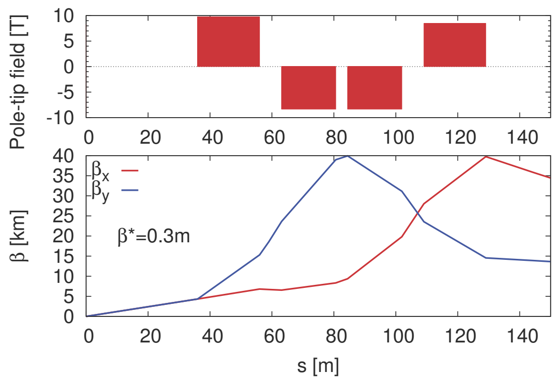

Figure 6: "Pushed" IR optics with $\beta^* = 0.3$ m and a free length $L^*= 36$ m.

Indeed, one important novel feature of FCC-hh is the high SR power, which is close to 2.4 MW per beam (at a beam current of 0.5 A) to be contrasted with 3.6 kW at the LHC. This power translates into a baseline heat load per meter and aperture of about 30 W/m/aperture, which could be absorbed on a beam screen (BS) inside the cold magnets as for the LHC, but at a higher BS temperature than the LHC's 5–20 K, in order to minimize the total refrigerator power [16]. Raising the BS temperature improves the Carnot efficiency for heat removal, but it also increases the heat radiation from the BS onto the cold bore of the magnets. The BS temperature which maximizes the total cooling efficiency increases as a function of SR heat load. At SR levels of 10–40 W/m the optimum is found at 50–100 K [17]. On the other hand, the warmer the BS, the larger is its resulting beam impedance.

Counteracting the radiation damping, during physics runs a continuous longitudinal and transverse noise excitation needs to be applied to keep the bunch length constant (preventing both component heating and instabilities) and to avoid excessive beam-beam tune shifts [18]. The controlled slow decrease of the transverse emittance, in proportion to the intensity decay, would allow for a dynamic β^* squeeze maximizing the integrated luminosity.

The total energy stored in the high-field magnets may exceed 100 GJ, while each of the two 50 TeV proton beams contains about 8 GJ. The systems for machine protection, beam dump, and collimation must be laid out accordingly.

4. Lepton Collider

Major challenges are designing an interaction region with 1.5–2.0% momentum acceptance; achieving a vertical-to-horizontal emittance ratio of 0.1% with colliding beams; and minimizing the cost while maximizing the efficiency of the SRF system.

Due to the unavoidable radiative Bhabha scattering the typical beam lifetime at the FCC-ee is about 40 times shorter than for LEP2 as a result of the much higher luminosity. The short beam lifetime, of less than one hour, can be counteracted by top-up injection, a scheme which has successfully been used at the KEKB and PEP-II B factories. Top-up injection allows operating the collider at constant magnetic field and with almost constant beam current, thereby avoiding magnet cycles and thermal transients, and greatly facilitating the optics tuning of the accelerator for optimum performance. Top-up injection requires a full-energy injector, i.e. with an energy of up to 175 GeV at least, which can be installed in the same 100-km tunnel as the collider.

The FCC-ee collider is conceived as a double ring with separate beam pipes for the two counterrotating lepton beams. This avoids parasitic collisions and, thereby, permits operation with a large number of bunches.

The synchrotron radiation power per beam is $P_{\rm SR} = (4\pi/3)(r_e/(m_e c^2)^3)E^4_{\rm beam} f_{\rm rev} n_b N_b/\rho$. The FCC design assumes a constant SR power of 50 MW per beam

Beamstrahlung, i.e. synchrotron radiation emitted during the collision in the field of the opposing beam, increases the steady-state energy spread and bunch length [19, 20]. Its high-energy tail may also limit the beam lifetime [21, 22], if beam particles which lose a significant fraction of their energy fall outside of the relative momentum acceptance $\delta_{\rm acc}$. Momentum acceptance is dominated by the IR design. Two first exploratory IR designs from CERN and BINP are described in the following.

4.1. CERN IR design

The CERN interaction region is shown in Fig. 7 together with the optical functions. It consists of a Final Focus System (FFS), Vertical and Horizontal Chromatic Correction Sections (CCSV, CCSH) and a Matching Section (MS). Currently the CERN design is sill in a very early stage of development and only the $t\bar{t}$ settings have been matched. The last drift, L^*, should be as small as possible while still leaving enough space to host the detector. At this stage of the design, $L^* = 2$ m is considered reasonable. Quadrupole design studies for SuperB suggest a minimum crossing angle of 11 mrad, which is used in the current CERN design.

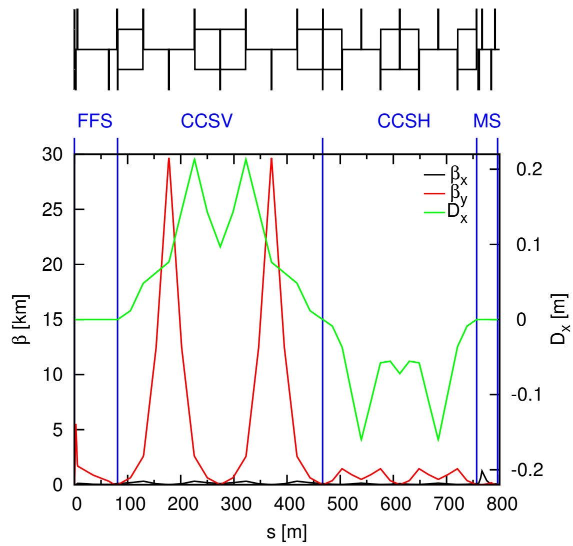

Figure 7: Optical functions of the CERN IR design.

4.2. BINP IR design

The philosophy of the BINP interaction region design is to apply a crab waist collision scheme [23] in order to increase Luminosity at low energies (Z,W). However, at high energies (H, $t\bar{t}$) the crab waist scheme has no considerable advantages since the beam-beam tune shift, and thereby the Luminosity, is limited by beamstrahlung. The BINP crossing angle is 30 mrad.

The general layout [24] and the optical functions are shown in Fig. 8. Again, a Final focus system (FFS) and Vertical and Horizontal Chromaticity Correction Sections can be seen as well as a CRAB section providing the necessary phase advance and optical functions for the crab sextupoles. The Chromaticity Correction Sections are much shorter than in the CERN design but this advantage comes at the price of much stronger dipoles. To mitigate the effects of synchrotron radiation at the IP (background in the detector), the first dipole has a rather low magnetic field.

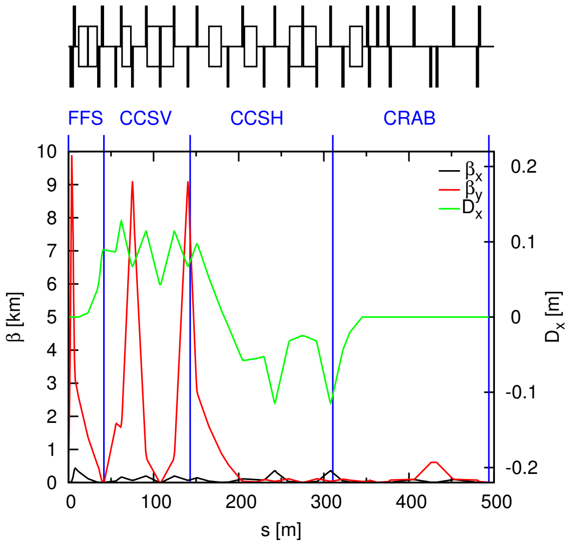

Figure 8: Optical functions of the BINP IR design.

4.3. Comparison and difficulties

In Fig. 9 the geometry of both FCC-ee designs are shown, together with the FCC-hh design for $L^* = 36$ m. Both FCC-ee designs require approximately the same tunnel diameter of about 2 m, which is reasonable.

Both BINP and CERN IR designs are incomplete since the two e^+/e^- lines need to be brought together and an RF section should also be included. First comparsions of synchrotron radiation are shown in Table 2. The BINP design radiates considerably more power than CERN design, more than 10 % of the overall Synchrotron radiation budget. Further studies are needed to determine how to shield this radiation.

First tracking calculations with the full 100 km arc lattice for high energies (Higgs, $t\bar{t}$) were conducted for both designs. All simulations were performed for on-momentum particles, 500 full turns with four IPs and without radiation by MADX and PTC. For these early studies the matching of arcs and interaction region was rather preliminary. The machines do not yet fully close and no RF section around the IR is included. The aim of these studies is to provide a first look at the dynamic aperture.

Table 2: Characteristics of the synchrotron radiation in the interaction regions.

	Z	**$t\bar{t}$**
Average total power per IP [kW]		
- CERN	138	138
- BINP	1460	1410
Energy loss per particle per IP [MeV]		
- CERN	0.8	168
- BINP	2.0	440
Average power in last dipole [kW]		
- CERN	7.3	7.3
- BINP	8.2	8.0
Critical Energy in last dipole [keV]		
- CERN	8.8	503
- BINP	20	1100

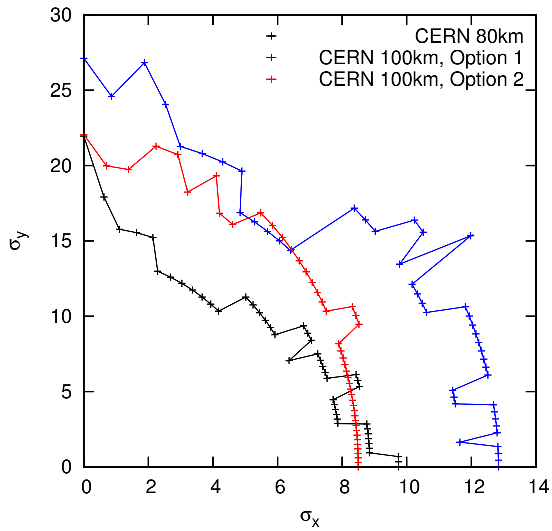

Figure 10: Dynamic apertures of the CERN design for 80 km option and two 100 km options at different working points.

The results for two different working points for the CERN IR are shown in Fig. 10 together with the earlier results with an 80 km arc lattice [25]. The largest dynamic aperture found so far is about 13σ in the horizontal plane and 25σ in the vertical plane.

Fig. 11 shows the tracking results for the BINP design at the 100 km option. It has a dynamic aperture of 8σ horizontaly and almost 100σ vertically. The latter is a very important property because the vertical beam size is considerably smaller than the horizontal.

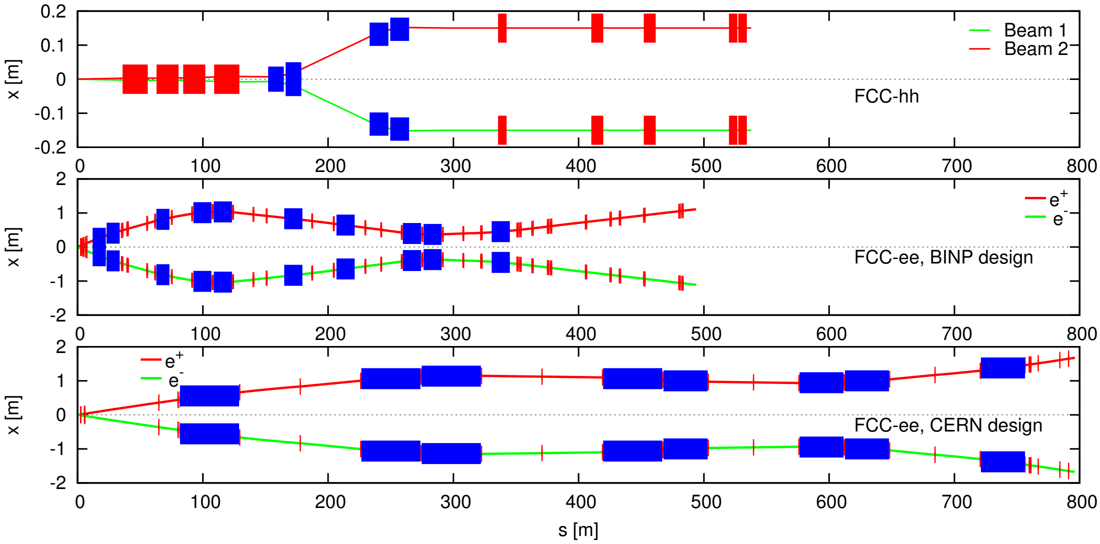

Figure 9: Comparison of the geometry of the current FCC-hh design and both FCC-ee designs. Dispersion suppressors are not included. Red rectangles represent quadrupoles, blue rectangles dipoles. Note the different scales for hadron and electron machines.

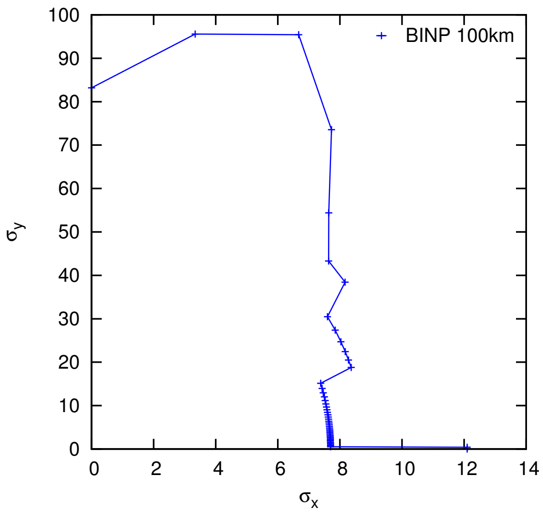

Figure 11: Dynamic aperture of the BINP design for the 100 km option.

References

[1] `http://cern.ch/fcc`

[2] A. Blondel, F. Zimmermann, arXiv:1112.2518v1 (2011).

[3] K. Oide, "SuperTRISTAN: A possibility of ring collider for Higgs factory", KEK Seminar, 13 February 2012.

[4] F. Zimmermann et al, "A High Luminosity e^+e^- Collider in the LHC Tunnel to Study the Higgs Boson", IPAC'12; A. Blondel, et al, arXiv:1208.0504 (2012).

[5] A. Blondel et al., CERN-ATS-2013-032, arXiv:1302.3318.

[6] K. Oide, F. Zimmermann, "The Circular Road to a Higgs Factory and Beyond", CERN-ACC-2013-0228 (2013).

[7] M. Bicer et al., "First look at the physics case of TLEP," JHEP 01, 164 (2014).

[8] M. Syphers, "SSC design considerations", FCC general meeting, May 2014. `https://indico.cern.ch/event/317384/`

[9] SSC Central Design Group, "Conceptual Design of the Superconducting Super Collider," SSC-SR-2020 (1986).

[10] R. Tomás et al, "Record low beta beating in the LHC", Phys. Rev. ST Accel. Beams **15**, 091001, 2012.

[11] E. Todesco et al, "The magnetic model of the LHC in the early phase of beam commissioning", CERN-ATS-2010-154.

[12] J. Serrano and M. Cattin. "The LHC AC dipole system: an introduction", CERN BE Note-14-CO, 2010.

[13] R. Tomás, "Adiabaticity of the ramping process of an ac dipole", Phys. Rev. ST Accel. Beams **8**, 024401, 2005.

[14] E. Todesco, L. Bottura, G. De Rijk, L. Rossi, "Dipoles for High-Energy LHC", MT-23, IEEE Trans. Appl. Supercond. 24, 2014.

[15] G. Battistoni et al., "The FLUKA code: Description and benchmarking", AIP Conf. Proc. 896 (2007) 31-49; A. Ferrari et al., "FLUKA: A multi-particle transport code (Program version 2005)", CERN-2005-010.

[16] D. Delikaris, L. Tavian, "Heat Loads and Cryogenics for HE-LHC", CERN-2011-003 (2011).

[17] P. Lebrun, private communication; D. Schulte, FCC Kick-Off, 13 February 2014.

[18] O. Dominguez, PhD thesis EPFL Lausanne, published in Editorial Series on Accelerator Science and Technology, (EuCARD Monograph), Warsaw University of Technology, no. 23, 2014.

[19] K. Yokoya, "Scaling of High-Energy e+e- Ring Colliders," KEK Accelerator Seminar, 15 March 2012.

[20] K. Ohmi, F. Zimmermann, "FCC-ee/CepC Beam-Beam Simulations with Beamstrahlung," THPRI004, IPAC14.

[21] V. Telnov, "Restriction on the energy and Luminosity of e^+e^- Storage Rings due to Beamstrahlung," PRL 110, 114801 (2013).

[22] A. Bogomyagkov, E. Levichev, D. Shatilov, PRST-AB 17, 041004 (2014).

[23] P. Raimondi, 2nd SuperB Workshop, Frascati, Italy, 2006

[24] A. Bogomyagkov, E. Levichev, P. Piminov, "Interaction Region Lattice for FCC-ee (TLEP)", THPRI008, IPAC'14.

[25] H. Garcia, L. Medina, R. Tomas, "FCC-ee Final Focus with Chromaticity Correction", THPRI010, IPAC'14.